Available online at www.sciencedirect.com

SciVerse ScienceDirect

Ceramics International 39 (2013) 6063–6068

CERAMICS INTERNATIONAL

www.elsevier.com/locate/ceramint

Giant dielectric permittivity and non-linear electrical behavior in $CaCu_3Ti_4O_{12}$ varistors from the molten-salt synthesized powder

Yanmin Huang[a,b,c], Laijun Liu[a,b,c,e,*], Danping Shi[a,b,c], Shuangshuang Wu[a,b,c], Shaoying Zheng[a,b,c], Liang Fang[a,b,c,e], Changzheng Hu[a,b,c,e], Brahim Elouadi[d]

[a]*State Key Laboratory Breeding Base of Nonferrous Metals and Specific Materials Processing, Guilin University of Technology, Guilin 541004, China*
[b]*Key Laboratory of New Processing Technology for Nonferrous Metal and Materials, Ministry of Education, Guilin University of Technology, Guilin 541004, China*
[c]*College of Material Science and Engineering, Guilin University of Technology, Guilin 541004, China*
[d]*Laboratoire de sciences de l'Ingénieur pour l'Environment, avenue michel crépeau, 17042 La Rochelle Cédex 01, France*
[e]*Guangxi New Future Information Industry Co., LTD, Beihai 536000, China*

Received 1 November 2012; received in revised form 9 January 2013; accepted 9 January 2013
Available online 17 January 2013

Abstract

$CaCu_3Ti_4O_{12}$ (CCTO) powder has been prepared by a molten salt method using the NaCl–KCl mixture. Crystal structure and microstructure of the powder and the resulting ceramics have been characterized by using X-ray diffraction (XRD) and scanning electron microcopy (SEM). Impedance analyzer and current–voltage meter were employed to analyze dielectric and nonlinear (*I–V*) properties of the CCTO ceramics with different sintering durations and subsequent cooling rates. The values of dielectric permittivity and nonlinear coefficient of the quenched sample were found to be higher than those of the slowly cooled sample. More specifically, the cooling methods (quenching and furnace-cooling) have allowed to adjust; (i) the breakdown voltage within a rather low range of 0.3–4.4 kV cm^{-1}; (ii) the nonlinear coefficient between 2 and 6 and (iii) the giant dielectric permittivity for the ceramics within a range from 5000 to 20000. A double Schottky barrier can be evidenced from the linear behavior between the ln *J* and $E^{1/2}$ in grain boundary regions. The relationship between the electrical current density and the applied electrical field indicates that the potential barrier height Φ_B is holding time dependent.

Keywords: B. Grain boundaries; C. Dielectric properties; $CaCu_3Ti_4O_{12}$; Varistors

1. Introduction

$CaCu_3Ti_4O_{12}$ (CCTO) ceramics have recently received considerable interest due to their exceptionally high dielectric permittivity (up to 10^5 at room temperature), which is independent of temperature in the range 100–600 K and in the frequency range10^2–10^6 Hz [1–3]. Furthermore, an extrinsic mechanism based on internal barrier layer capacitor (IBLC) effect is widely accepted to explain the giant dielectric properties of CCTO ceramics [4–7]. In addition to the high permittivity, we have also evidenced remarkably nonlinear current–voltage (*I–V*) characteristics of CCTO ceramics, which makes it suitable for the varistor application [8–10].

Furthermore, it was found that dielectric properties and *I–V* behavior of CCTO are very sensitive to fabrication process [11,12]. For example, Chen et al. [13] have reported that CCTO ceramics from molten-salt synthesized powders, whose synthesis temperature can be decreased as low as 750 °C for NaCl–KCl eutectic mixture as the flux, showed a high dielectric permittivity and a very low loss factor. While Nahm [14] demonstrated that nonlinear electrical properties of such ceramics can be controlled by changing the sintering temperature or cooling process [14]. Therefore, it appeared to us of interest to carry out a systematical investigation of giant dielectric and *I–V*

*Corresponding author at: College of Material Science and Engineering, Guilin University of Technology, Guilin 541004, China.
Tel.: +86 77 35893395; fax: +86 77 35896290.
E-mail address: ljliu2@163.com (L. Liu).

0272-8842/$ - see front matter © 2013 Elsevier Ltd and Techna Group S.r.l. All rights reserved.
http://dx.doi.org/10.1016/j.ceramint.2013.01.023

behavior under various conditions of thermal treatment based on the grain boundary characteristic. The purpose of the present work is to correlate the physical properties to the processing via modifying the grain boundary behavior of the CCTO ceramics by different cooling methods (water-quenching and furnace-cooling). A double Schottky barrier model is employed to explain the giant dielectric and nonlinear *I–V* behavior.

2. Experimental

$CaCu_3Ti_4O_{12}$ (CCTO) ceramics were elaborated by a molten salt synthesis method. The stoichiometric mixture of the starting materials $Ca(NO_3)_2 \cdot 4H_2O$, $Cu(NO_3)_2 \cdot 3H_2O$ and TiO_2 were ground before being added to the eutectic composition (44NaCl–56KCl), which melts at about 657 °C. The starting compounds and the chloride salts were mixed in a ball mill using zirconia's balls as milling medium in ethanol for 12 h. The mixture with a mass ratio [CCTO/salt]=0.3 were heated in a high purity alumina crucible at 800 °C for 1 h. After being slowly cooled to room temperature, the obtained product was washed in hot deionized water until a total dissolving (detected by silver nitrate) of all chloride was achieved. The washing process was repeated for about twenty times. The resultant powder was oven-dried at 105 °C for 4 h prior to the characterization. The obtained CCTO powder was pressed into pellets of ~13 mm diameter and ~1 mm thickness by a cold isostatic pressing method. Two pellets were successively sintered at 1060 °C for 1 h and 3 h, and were cooled in furnace, leading to samples CCTO-1h and CCTO-3h, respectively. Another one with dwelling 3 h at 1060 °C was quenched in water, leading to sample CCTO-3hQ.

X-ray diffraction patterns were recorded at room temperature using (X'Pert PRO) X-ray diffractometer with Cu Kα radiation (λ=1.5406 Å). Furthermore, scanning electron microscopy (SEM, JEOL, JSM-5610, Japan) was used to examine the grain morphology for the powder. Furthermore, the cross section morphology of the CCTO ceramics was characterized by using SEM (JSM-6380LV) at 15 kV. The samples were coated with a carbon film prior to the SEM experiments. In order to analyze the electrical prosperities of the material, both sides of the ceramics samples were polished and then coated with silver conductive paste followed by a heating treatment at 650 °C for 30 min in order to ensure good electrical contact. Dielectric characteristics were performed using an impedance analyzer (Agilent 4294 A) over the frequency range 40 Hz–100 MHz with applied voltage of 500 mV at room temperature (RT). The nonlinear current-voltage behavior of the CCTO ceramics was analyzed using a high voltage measurement unit (Model 610E, TREK). The source voltage was raised with a rate of 4 V s^{-1} while the measurements were performed at temperatures of 25 °C, 40 °C, 55 °C and 70 °C, which was kept constant with an accuracy of ±1 °C.

3. Results and discussion

XRD patterns of the CCTO powder and resulting ceramics are given in Fig. 1. The powder heated at 800 °C for 1 h contains the main phase CCTO [ICDD PDF Card no. 21-0140] and minor phases CuO, TiO_2 and $CaTiO_3$. While the ceramics with different dwelling times and cooling processes are pure perovskite phase [ICDD PDF Card No. 21-0140], which all peaks can be indexed according to cubic crystal structure with *Im-3* space group.

SEM images of CCTO powder and ceramics are shown in Fig. 2. As evidenced in Fig. 2(a), the powder is characterized by agglomerated grain with sizes smaller than 1 μm. However, as shown in Fig. 2b, the grain of CCTO ceramic grows significantly just after 1 h sintering. Furthermore, the ceramic is composed of large and small grains, and the size of larger grains is ~16 μm while that of smaller grains is ~3 μm. After further heating for 3 h, the size of bigger grains does not change significantly but the number of smaller grains decreases (Fig. 2c). The morphology of CCTO ceramics cooled with different methods is shown in Fig. 2c and d. It can be seen that the morphology of ceramic grains and grain size are not affected much by the cooling rate (furnace-cooling or water-quenching). Different fracture mechanisms present in the CCTO-3h and CCTO-3hQ, however, a transgranular fracture happens in the CCTO-3h while an intergranular fracture in the CCTO-3hQ. It suggests the grain boundary characteristic of them is different. The density of ceramics CCTO-1h, CCTO-3h and CCTO-3hQ are equal to 4.95, 4.98 and 4.97 g cm^{-3}, respectively. These values are very close to the one determined from the lattice data (5.0 g cm^{-3}) of pure CCTO.

The frequency dependence of dielectric permittivity (ε_r) and loss factor ($\tan\delta$) for CCTO-1h, CCTO-3h and CCTO-3hQ are represented in Fig. 3(a) and (b), respectively. It can be seen that both ε_r and $\tan\delta$ are very

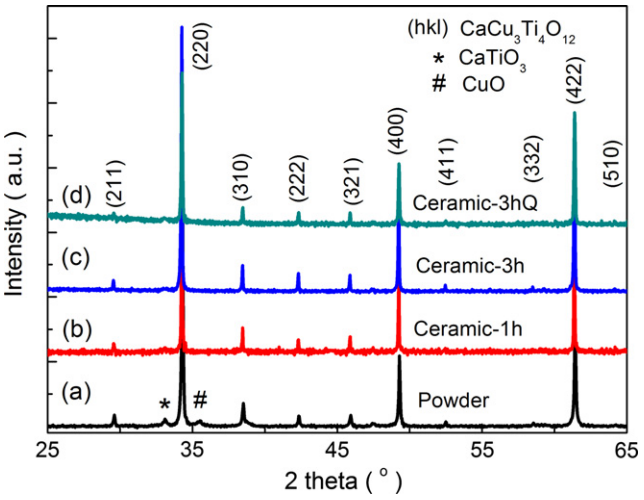

Fig. 1. X-ray diffraction patterns of the CCTO powder synthesized by the molten salt method and the resulting ceramics: (a) powder synthesized by the molten salt method, (b) CCTO-1h, (c) CCTO-3h and (d) CCTO-3hQ.

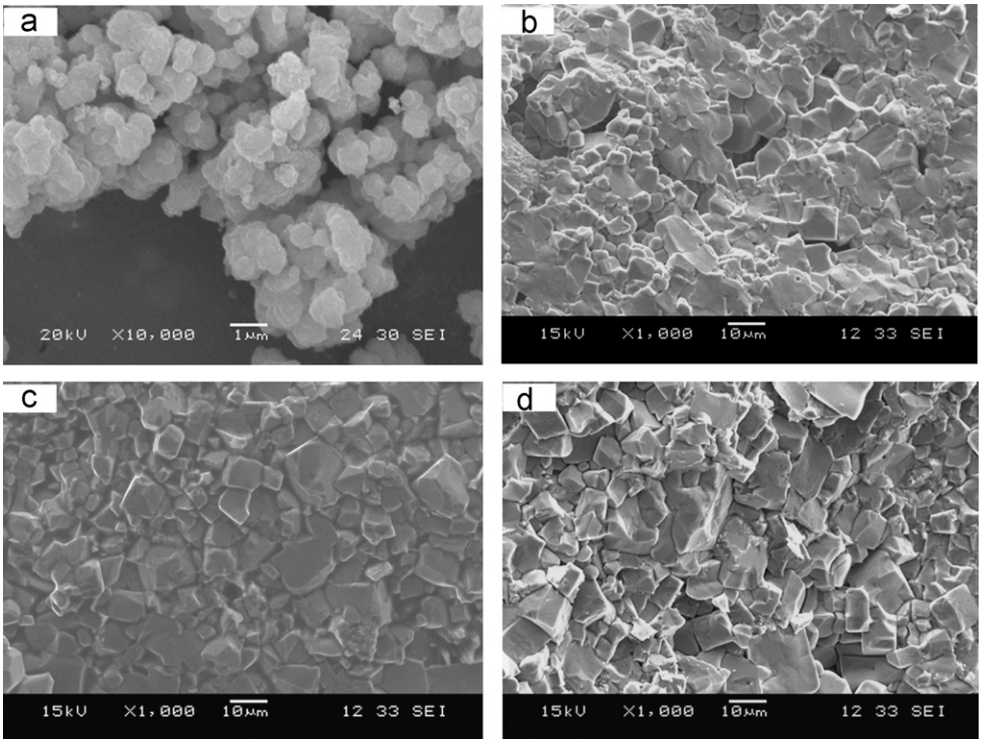

Fig. 2. SEM images of the CCTO powder and the resulting ceramics: (a) powder synthesized by the molten salt method, (b) CCTO-1h, (c) CCTO-3h and (d) CCTO-3hQ.

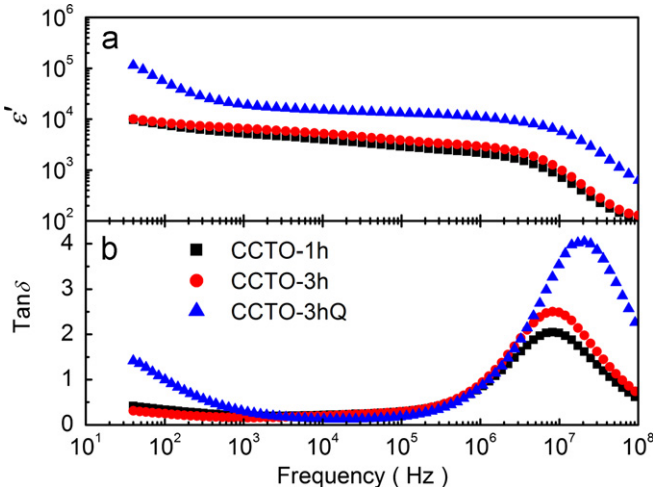

Fig. 3. Frequency dependence of dielectric constant (ε') and dielectric loss tangent ($\tan\delta$) for the CCTO ceramics measured at room temperature.

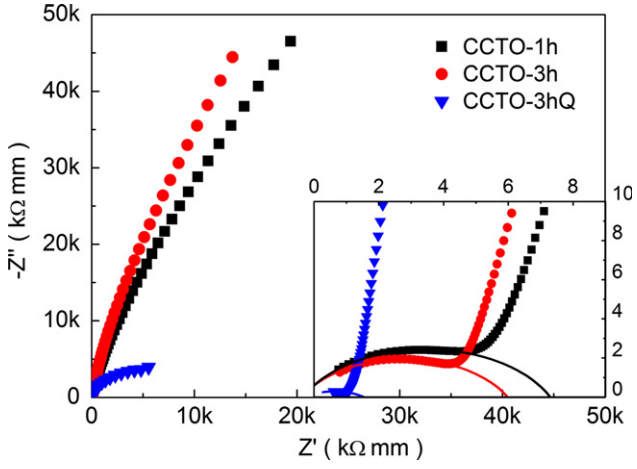

Fig. 4. Impedance complex plane plots of the CCTO ceramics at room temperature. The inset shows an expanded view of the high frequency data close to the origin, the fitting curves are based on a RC parallel circuit.

sensitive to the thermal history of the ceramics: (i) the value of ε_r and $\tan\delta$ tend to increase with increasing sintering time; (ii) the peak of $\tan\delta$ (f) and the related inflexion points of ε_r (f) are displaced to higher frequency domain with increasing sintering time; (iii) the differences between the $\tan\delta$ plots is mainly observable in low ($f < 10$ kHz) and high ($f > 2$ MHz) frequency ranges. It is worth to notice that the three investigated ceramics display the Debye relaxation behavior [15]. The relaxation characteristic can be identified by impedance spectroscopy.

Impedance spectroscopy is a powerful technique for unraveling the complexities of materials, e.g. electrically inhomogeneous structure containing semiconducting grains with insulating grain boundary regions [16]. Fig. 4 shows impedance plots of the CCTO ceramics at RT. Each complex impedance plot shows two semicircles: one in the high frequency range is associated with grain response (Fig. 4 insert); while the other one is related to grain boundary response at low frequencies. Resistance of grains decreases slightly with increasing dwelling time while it is

significantly restrained for water-quenching process (see the curves fitting based on a RC parallel circuit in Fig. 4 insert). The semi-conductivity of the grains arises from a small amount of oxygen-loss (oxygen vacancy) occurred in high temperature sintering procedure in the CCTO ceramics. Prolonged dwelling time for the CCTO ceramics can enhance the creation of oxygen vacancy in grains. Especially, a large number of oxygen vacancies are expected to be frozen at room temperature for the water-quenched sample. While cooling in furnace from high temperature would allow limited reoxidation to occur along grain boundary regions and generate an electrical microstructure consisting of semiconducting grains and insulating grain boundaries.

Nonlinear current–voltage (I–V) characteristic is closely correlated with grain boundary behavior in the CCTO ceramics. I–V responses of the CCTO-1h, CCTO-3h and CCTO-3hQ measured at different temperatures are shown in Fig. 5. The nonlinear behavior of the current density (J) to the applied electric field (E) is given by the equation $J=kE^{\alpha}$ similar to varistors [17]. The nonlinear coefficient (α) gives the degree of non-linearity; the constant k depends on the microstructure and is related to the electrical resistivity of materials. A breakdown electric field (threshold electric field) (E_b) is defined as the electric field intensity at a current density of 1 mA cm^{-2} in this experiment. The breakdown voltages (E_b) and nonlinear coefficients (α) obtained from the plots are shown in Table 1. Breakdown voltage of the CCTO-1h 4.37 kV cm^{-1} is higher than that of Zhang et al. [18] (about 1 kV cm^{-1}) and Cheng et al. (0.32 kV cm^{-1}) [19]. Generally, breakdown voltages fall off as measure temperature increases. The CCTO-1h sample shows the highest nonlinear coefficient and breakdown voltage, which indicates that the sample contains the widest grain boundary thickness. However, so high breakdown voltage makes it does not meet the requirement of automatic control circuits and semiconductor circuits. Therefore, CCTO-3hQ could be considered as a promising material for application in microelectronics, especially in capacitive components and varistors.

The I–V characteristic of CCTO ceramic varistors should also be associated with grain boundaries and correlated barrier height. Normally, a double Schottky barrier is created in electroceramics between grains and grain boundaries while grain boundaries act as an extrinsic

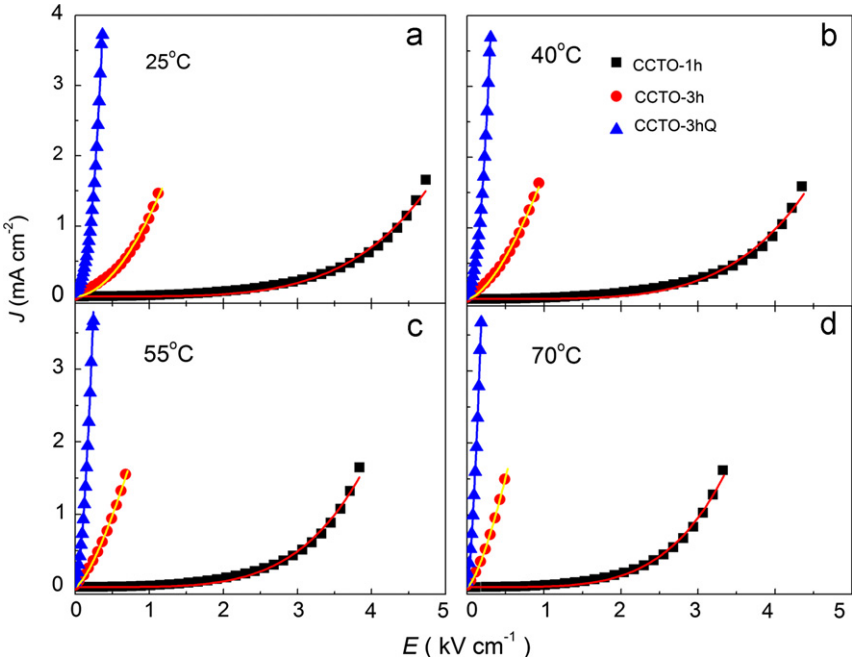

Fig. 5. Current density (J)–electric field (E) plots for the three different CCTO ceramic samples at different temperatures, (a) 25 °C, (b) 40 °C, (c) 55 °C and (d) 70 °C. The solid line is fitted by $J=kE^{\alpha}$.

Table 1
The nonlinear coefficient (α) and breakdown voltages (E_b) of CCTO ceramics at different temperatures.

Samples	25 °C		40 °C		55 °C		70 °C	
	α	E_b (kV cm^{-1})	α	E_b (kV cm^{-1})	α	E_b (kV cm^{-1})	α	E_b (kV cm^{-1})
CCTO-1h	5.87	4.37	6.21	4.05	5.71	3.54	5.36	3.05
CCTO-3h	2.01	0.94	1.81	0.71	1.50	0.52	1.48	0.38
CCTO-3hQ	2.48	0.21	2.20	0.17	1.80	0.11	1.55	0.076

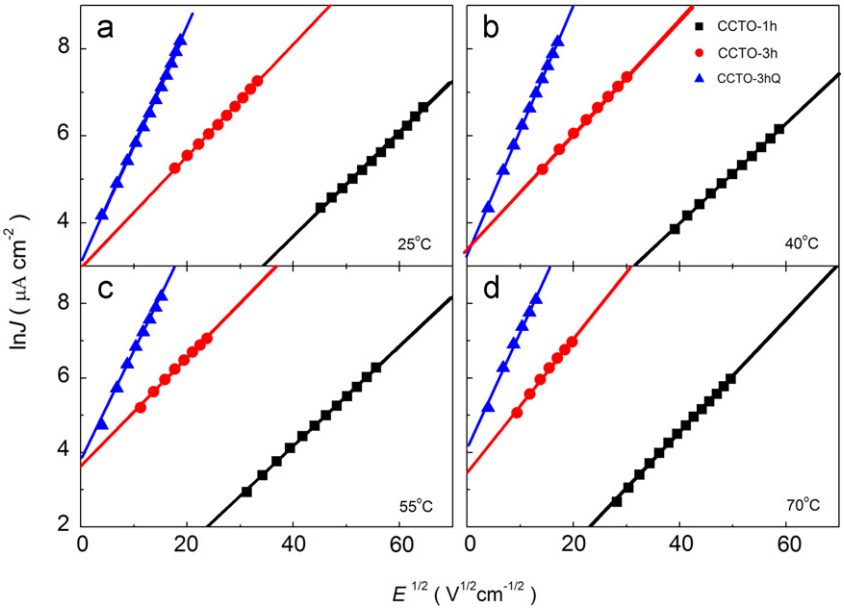

Fig. 6. Plots of ln J versus $E^{1/2}$ for the three different CCTO ceramic samples at different temperatures, (a) 25 °C, (b) 40 °C, (c) 55 °C and (d) 70 °C.

source of impedance. Thus, by considering the potential barriers in CCTO varistors to be of a Schottky type, the electrical conduction in the pre-breakdown region should be associated with the thermion emission of the Schottky type and depends on the temperature and electric field. Therefore, the electrical current density (J) and the applied electrical field (E) will follow the relationship [20–22]

$$J = AT^2 \exp\left(\beta \frac{E^{1/2} - \phi_B}{k_B T}\right) \quad (1)$$

$$\ln J_0 = \ln AT^2 - \frac{\phi_B}{k_B T} \quad (2)$$

where A is the Richardson constant, k_B is the Boltzmann constant, Φ_B is the electrical potential barrier height formed at the interface region, and β is a constant related to the potential barrier width. J_0 is the extrapolated value to $E=0$.

According to the Schottky conduction model, the plots of ln J against $E^{1/2}$ for the CCTO ceramics is used to determine the potential barrier height at the low current density range. The electrical current density (J) versus the electrical field (E) was measured at various temperatures, as shown in Fig. 6, a good linear relationship between ln J and $E^{1/2}$ can be obtained, which indicates that the Schottky barrier should exist at grain boundary regions. J_0 data are obtained as the curves are extrapolated to $E=0$. Then, we plot the curves of ln J_0 versus $1000/T$, as shown in Fig. 7, a good linear behavior can also be obtained, which indicates that the variation in the pre-exponential term of Eq. (2) with temperature is very small. Therefore, the potential barrier height Φ_B, derived from the slope of the plots, is 0.47 eV, 0.40 eV and 0.39 eV for CCTO-1h, CCTO-3h and CCTO-3hQ, respectively. The values are similar to the results of Cheng et al. [19] (0.53 eV) and Lu et al. [23] (0.60 eV). Therefore, the reoxidation of grain boundaries makes important influence on the barrier height. In addition, the breakdown voltage is closely correlated to the barrier height, which is associated with intrinsic defects, such as oxygen vacancies, at grain boundaries.

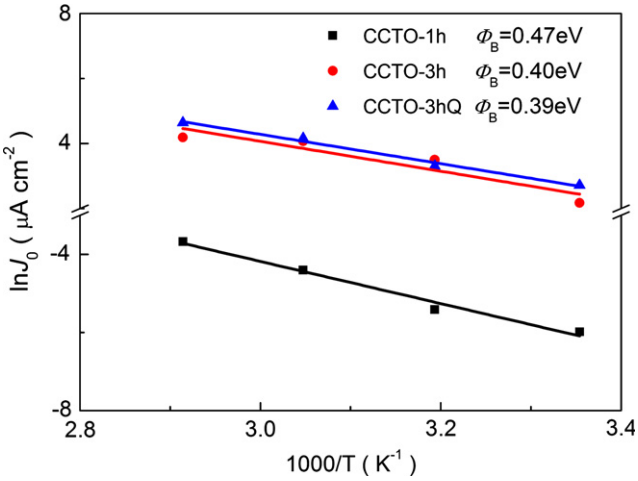

Fig. 7. Plots of ln J_0 versus $1000/T$ of the CCTO ceramics. The solid line is fitted by Eq. (2).

4. Conclusions

Giant dielectric permittivity and good nonlinear I–V CCTO varistors were successfully prepared by a molten salt synthesis method. The dielectric properties and nonlinear I–V characteristic can be modified by sintering time and cooling process. The relationship between current density versus applied electrical field indicates that the activation energy of grain boundaries of CCTO varistors is almost similar to the potential barrier height. CCTO-3hQ

could be considered as a promising material for application in microelectronics as varistors due to its high dielectric constant and nonlinear coefficient and low breakdown voltage.

Acknowledgments

This work was supported by the Natural Science Foundation of China (Nos. 11264010, 51002036, 50962004, 21061004 and 51102058), the Project of Department of Scicence and Technology of Guangxi (Nos. 12118017-13, 10-046–01, 11-031-03 and 11107006-42), the Natural Science Foundation of Guangxi (Grant no. BA053007) and by the Program for Excellent Talents in Guangxi Higher Education Institutions.

References

[1] A.P. Ramirez, M.A. Subramanian, M. Gardel, G. Blumberg, D. Li, T. Vogt, S.M. Shapiro, Giant dielectric constant response in a copper–titanate, Solid State Communications 115 (2000) 217–220.
[2] M.A. Subramanian, D. Li, N. Duan, B.A. Reisner, A.W. Sleight, High dielectric constant in $ACu_3Ti_4O_{12}$ and $ACu_3Ti_3FeO_{12}$ phases, Journal of Solid State Chemistry 151 (2000) 323–325.
[3] J.C. Zhao, J. Liu, G. Ma, Preparation, characterization and dielectric properties of $CaCu_3Ti_4O_{12}$ ceramics, Ceramics International 38 (2012) 1221–1225.
[4] L. Zhang, Z.J. Tang, Polaron relaxation and variable-range-hopping conductivity in the giant-dielectric-constant material $CaCu_3Ti_4O_{12}$, Physical Review B 70 (2004) 174306.
[5] A.R. West, T.B. Adams, F.D. Morrison, D.C. Sinclair, Novel high capacitance materials: $BaTiO_3$: La and $CaCu_3Ti_4O_{12}$, Journal of the European Ceramic Society 24 (2004) 1439.
[6] G. Chiodeli, V. Massarotti, D. Capsoni, M. Bini, C.B. Azzoni, M.C. Mozzati, P. Lupotto, Electric and dielectric properties of pure and doped $CaCu_3Ti_4O_{12}$ perovskite materials, Solid State Communications 132 (2004) 241–246.
[7] P. Lunkenheimer, S. Krohns, S. Riegg, S.G. Ebbinghaus, A. Reller, A. Loidl, Colossal dielectric constants in transition-metal oxides, European Physical Journal: Special Topics 180 (2010) 61–69.
[8] S.Y. Chung, I.D. Kim, S.J.L. Kang, Strong nonlinear current–voltage behaviour in perovskite-derivative calcium copper titanate, Nature Materials 3 (2004) 774–778.
[9] L.J. Liu, L. Fang, Y.M. Huang, Y.H. Li, D.P. Shi, S.Y. Zheng, S.S. Wu, C.Z. Hu, Dielectric and nonlinear current–voltage characteristics of rare-earth doped $CaCu_3Ti_4O_{12}$ ceramics, Journal of Applied Physics 110 (2011) 094101.
[10] L.J. Liu, Y.M. Huang, Y.H. Li, D.P. Shi, S.Y. Zheng, S.S. Wu, L. Fang, C.Z. Hu, Dielectric and non-ohmic properties of $CaCu_3Ti_4O_{12}$ ceramics modified with NiO, SnO_2, SiO_2, and Al_2O_3 additives, Journal of Materials Science 47 (2012) 2294–2299.
[11] R.N.P. Choudhary, U. Bhunia, Structural, dielectric and electrical properties of $ACu_3Ti_4O_{12}$ (A = Ca, Sr and Ba), Journal of Materials Science 37 (2002) 5177–5182.
[12] T.B. Adams, D.C. Sinclair, A.R. West, Giant barrier layer capacitance effects in $CaCu_3Ti_4O_{12}$ ceramics, Advanced Materials 14 (2002) 1321–1323.
[13] K.P. Chen, X.W. Zhang, Synthesis of calcium copper titanate ceramics via the molten salts method, Ceramics International 36 (2010) 1523–1527.
[14] C.W. Nahm, Effect of cooling rate on electrical properties, impulse surge and dc-accelerated aging behaviors of ZPCCD-based varistors, Journal of Materials Science: Materials in Electronics 20 (2009) 418–424.
[15] L. Liu, H. Fan, L. Wang, X. Chen, P. Fang, Dc-bias-field-induced dielectric relaxation and ac conduction in $CaCu_3Ti_4O_{12}$ ceramics, Philosophical Magazine 88 (2008) 537–545.
[16] D.C. Sinclair, T.B. Adams, F.D. Morrison, $CaCu_3Ti_4O_{12}$: one-step internal barrier layer capacitor, Applied Physics Letters 80 (2002) 2153–2155.
[17] D.R. Clarke, Varistor ceramics, Journal of the American Ceramic Society 82 (1999) 485–502.
[18] Q.L. Zhang, T. Li, Z.P. Chen, R.Z. Xue, Y.Q. Wang, The non-ohmic and dielectric behavior evolution of $CaCu_3Ti_4O_{12}$ after heat treatments in oxygen-rich atmosphere, Materials Science and Engineering B 177 (2012) 168–172.
[19] B. Cheng, Y.H. Lin, J.C. Yuan, J.N. Cai, C.W. Nan, X. Xiao, J.L. He, Dielectric and nonlinear electrical behaviors of La-doped $CaCu_3Ti_4O_{12}$ ceramics, Journal of Applied Physics 106 (2009) 034111.
[20] S.A. Pianaro, P.R. Bueno, P. Olivi, E. Longo, J.A. Varela, Effect of Bi_2O_3 addition on the microstructure and electrical properties of the $SnO_2CoONb_2O_5$ varistor system, Journal of Materials Science Letters 16 (1997) 634–638.
[21] G. Zang, J. Zhang, P. Zheng, J. Wang, C. Wang, Grain boundary effect on the dielectric properties of $CaCu_3Ti_4O_{12}$ ceramics, Journal of Physics D: Applied Physics 38 (2005) 1824–1827.
[22] Y.J. Wang, J.F. Wang, C.P. Li, H.C. Chen, W.B. Su, W.L. Zhong, P.L. Zhang, L.Y. Zhao, Improved varistor nonlinearity via sintering and acceptor impurity doping, European Physical Journal Applied Physics 11 (2000) 155–158.
[23] Z.Y. Lu, X.M. Li, J.Q. Wu, Voltage–current nonlinearity of $CaCu_3Ti_4O_{12}$ ceramics, Journal of the American Ceramic Society 95 (2) (2012) 476–479.